

# Thermal Printing on Composite Media

William T. Vetterling\*

ZINK Imaging, Inc.

\*Corresponding author: 16 Crosby Drive, Bedford, MA 01730, william.vetterling@zink.com

**Abstract:** In direct thermal printing, media is exposed to heat pulses from a print head carrying a linear array of resistive heaters. The heaters are spaced along a cylindrical glass bump, and the bump is pressed against the surface of the media. It is important that the media be compressible so that it will wrap around the curved bump and contact the heaters over their entire length. In some cases, the choice of media substrate is restricted to materials that are not adequately compressible. In this study we investigate the degree to which a thin substrate can be combined with a thin compressible sub-layer to provide a composite structure that conforms adequately to the heaters.

**Keywords:** thermal printing, direct thermal, thermal print head, media, compressibility

## 1. Introduction

Direct thermal printing is a process in which a print medium is subjected to heating that initiates a chemical reaction and leads to a change in optical density. Traditional thermal FAX paper uses such a process, and has suffered the limitation that with a single control variable (i.e. temperature) it is impossible to address a full 3-dimensional color space. Thus, direct thermal printing has been restricted to the printing of a single color, usually black on a white background, or to a limited selection of colors that lie on a one-dimensional contour through the full 3D space of color. This limitation has been recently overcome by a method that combines temperature and thermal power level to allow addressing of the full color domain.<sup>1,2</sup>

This technology has allowed the development of direct thermal printers with photographic color. The printers incorporate a conventional thermal print head having a linear array of heater elements that are pressed against the media. (Figure 1). The heaters are located on a curved glass bump, and the media is normally supported from the rear by a rubber platen. The function of the rubber is to deform slightly, so as to wrap the media around the bump and to bring it in into

intimate contact with the full length of the heaters. In some applications, the use of a rubber platen is not possible (e.g. if the active coatings are applied directly to a solid object, or are part of a label that is pre-applied to such an object.) In these cases, the support does not normally have the properties necessary to wrap the media to the heaters, and successful printing comes to rely on the compressibility of the label itself.

Attempts have been made to use compliant voided substrates in this application, relying on the voids for compressibility. This approach is successful, but in some applications the dimensional stability of these voided substrates is inadequate. Therefore, we have also investigated the roll of an adhesive in constructing a layered structure with adequate conformability.

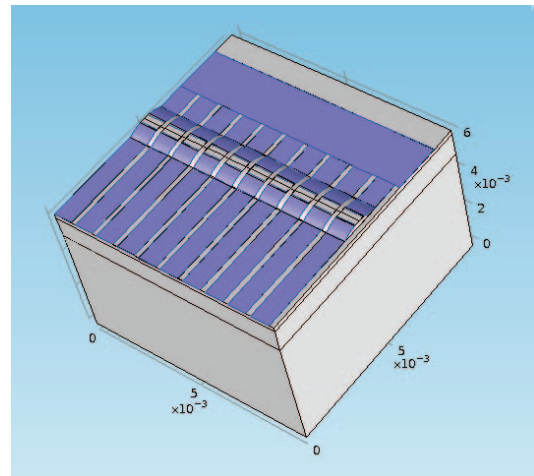


**Figure 1.** Schematic print-head segment containing 10 heaters on top of a cylindrical glass bump with a typical radius of curvature of 2-3 mm. Each heater has an individual electrical lead on one side, and connects to a common bus on the other.

## 2. Model Description

Figure 2 is a 3D view of the system model, showing a section of the glass bump compressing a layered media. The media

substrate properties are ideally similar to those of the object onto which the label is placed to reduce the risk that differential stresses (e.g. thermal expansion) will result in separation of the label from the object or damage to the label. Between the label and substrate is the layer of adhesive that we rely on for compressibility.

Mechanically, the system is not complicated, but some details require explanation.

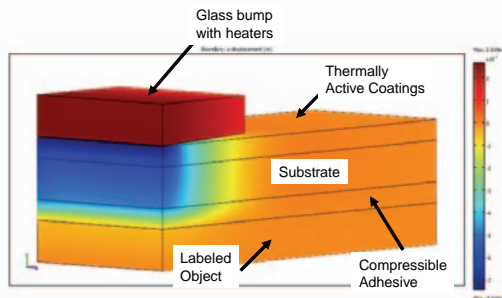


**Figure 2.** Representation of the model in three dimensions. A vertical compressive force is applied uniformly to the top surface of the glass bump, and the colors represent the strain-field that results.

The model is carried out with the COMSOL Multiphysics Structural Mechanics Module. The surface of the glass bump and the surface of the media are identified as a “contact pair”, so that deformation will occur when they are pressed together. The “contact parameter”, which identifies points of contact, was used to measure the *mechanical* contact-length between the print head and the media. However, this in itself is not a complete description of *thermal* contact.

When the head and media have a small enough separation, the air in the intervening gap has sufficient thermal conductivity to ensure that the temperature differential is also small and has negligible effect on the printing process. In this case, the two may be considered to be still in thermal contact, though not physically touching. Since the glass bump is tangent to the media at the point of contact, even the allowance for gaps of this small size may lead to results for thermal contact-length that are in some instances significantly larger than the corresponding results for mechanical contact-length. For the purposes of this study, we have taken *thermal*

contact-length to be defined by that region of the glass bump that has a gap of less than 0.1  $\mu\text{m}$  with the media. We have found that this measure of contact exhibits a better qualitative agreement with observations of print density than does the mechanical contact.

The calculation was initially conceived as a 2D problem, and Figure 3 illustrates a typical result from a 2D plane-strain calculation. With results of this type, we record the distance at which the gap first becomes non-zero, and the value is doubled (accounting for symmetry) to find the physical contact length. Similarly, we record the distance at which the gap becomes 0.1 microns and double it to find the thermal contact length. The recorded data may then be reported as in Figure 4, which shows a variation in mechanical and thermal contact lengths for a case in which the Young’s modulus of the adhesive is held at 100  $\mu\text{m}$  and that of the coatings is varied over a wide range.

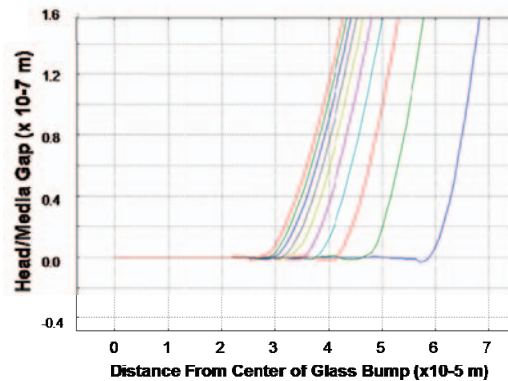


**Figure 3.** Typical results for the head-to-media gap as a function of the distance from center of the glass bump. The curves, from right to left, represent the results for  $Y_{\text{coatings}} = 100\text{-}1000$  MPa in steps of 100 MPa, with a fixed  $Y_{\text{adhesive}}$  of 100 MPa.

It was noted that plane-stress and plane-strain calculations differed by 20% in computed contact-lengths, and one must ask which of the two approximation more accurately represents the true 3D calculation. On the one hand, the applied stress from the glass bump is in the plane of a 2D cross-section of the model, and could be expected to cause an out-of-plane component of strain. On the other had, the external stress is applied to a long line on the surface of the media,

and substantial out-of-plane stress develops nearby to counteract the strain along that line. In fact, a symmetry argument suggests that the out-of-plane strain should be zero in the limit of an infinitely long print head.<sup>3</sup>

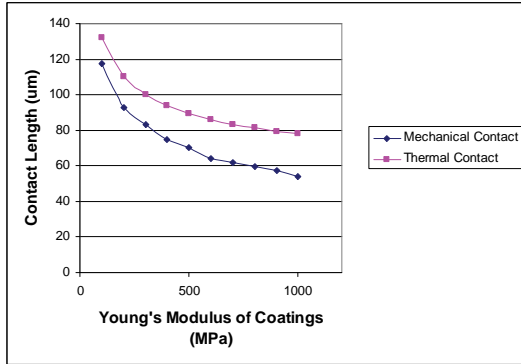


**Figure 4:** Mechanical (in blue) and thermal (in red) contact lengths as a function of the Young's modulus of the coatings.

The definitive method for resolving this issue is to perform a full 3D calculation, but a typical print head is several inches long, and some layer thicknesses in the media are just 25 um. The mesh for a full 3D model is therefore quite large. Instead, we modeled a narrow slice of the print head, and compared results with the 2D plane-stress and 2D plane-strain results as the width of the modeled slice was changed.

An arbitrary slice from the print head has two lateral walls on which the boundary conditions are not generally known. To deal with this we note that the full print head has a symmetry plane in the center and a free boundary at the ends (Figure 5). The modeled slice was likewise given a symmetry boundary condition on one lateral wall and a free boundary condition on the other. In effect, we are treating the slice as if it were one-half of a full print head of very narrow width, and observing the limiting behavior as the width is raised toward more realistic values. This limit is then taken as the correct “long-print head” result. It was observed that limiting values were approached for quite narrow slices (several hundred microns) so that it was never necessary to implement models larger width.

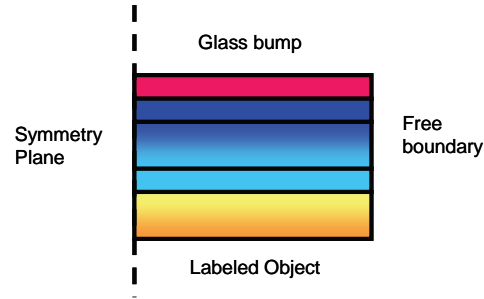


**Figure 5.** Boundary conditions for the two lateral faces of the model. The symmetry plane represents the center of the print head, and the free boundary represents one of the two ends

### 3. Results

This model has several parameters, and we shall present only a representative sample of the results. The nominal model parameters are listed in Table 1.

d_substrate	50e-6[m]	Thickness of substrate
d_adhesive	25e-6[m]	Thickness of adhesive
d_coatings	25e-6[m]	Thickness of coatings
Y_substrate	2.3[GPa]	Young's modulus, substrate
Y_adhesive	100[MPa]	Young's modulus, adhesive
Y_coatings	800[MPa]	Young's modulus, coatings
Y_glass	73.1[GPa]	Young's modulus, glass bump
r_bump	2e-3[m]	Radius of glass bump
F_head	39 [kg/m]	Head force/length

**Table 1.** Nominal parameter values used in this study, except as noted otherwise in the text and figures.

First, we explored the effect of the length of the modeled media segment in the direction perpendicular to the glaze bump and in the plane of the media layers (see Figure 6). This study was aimed at choosing a model length that adequately encompassed the strain field. It was found that models that included media up to 250 um to each side of the heater line produced results that were virtually identical to models of twice this length. Models of 150 um to each side, however, impinged too far into the strain field and gave significant errors. The modeled media length was therefore set at 250 um.

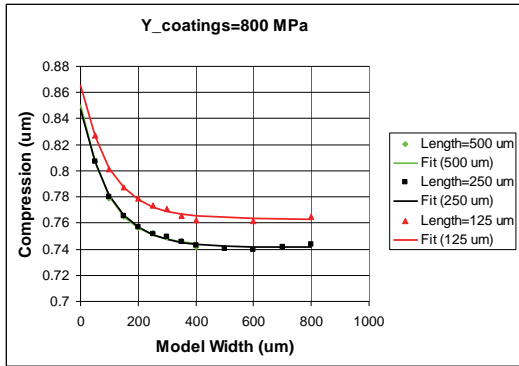


**Figure 6.** Compression vs. model width for three different down-web lengths. A length of 250 um includes a sufficient portion of the full strain field.

As a second step we modeled systems with lateral width up to 400 um, and observed the dependence of the compression at the center of the print head on the width of the modeled slice (Figure 7). The results fit accurately to a quadratic function of the modeled width. For very narrow slices, the extrapolated result matches a 2D plane stress calculation. For wider slices the results become more accurately represented by the 2D plane strain calculation, with an error of approximately 5% for positions more than a few hundred microns from the free ends of the print head.

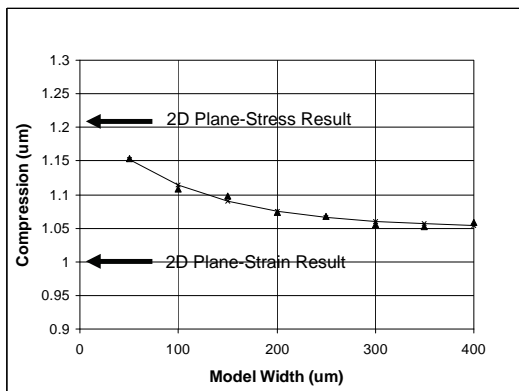


**Figure 7.** Variation of the media compression with model width. The 2D plane-stress result is accurate for narrow slices, but the 2D plane-strain result is more accurate for print heads of practical length.

In the model just described, the Young's modulus was 200 MPa for the coatings and 100 MPa for the adhesive. The study was repeated

using a higher value (800 MPa) for the Young's modulus of the coatings, and the results were qualitatively quite similar, both in the dependence on model width and in the relationship of the 3D result to the two 2D results. Consequently, we have concluded that a model width of about 200 um is generally adequate to obtain results within about 2% of the long-print head limit.

### 3.1 Uniform Adhesive

Having chosen a model width of 200 um and a model length of 250 um, we then inspected other features of the model.

As a practical matter, it is preferable to use thin substrates for labels, but it becomes increasingly difficult to coat on thin materials as the thickness falls below 100 um. Figure 8 shows the contact-length as a function of Y\_coatings using a substrate of 50 um thickness. The adhesive had a Young's modulus of 100 MPa. This study was repeated using a substrate thickness of 63 um, and the results were virtually identical. It was concluded that the dependence of contact on substrate thickness is not a strong one in the vicinity of 50-100 um, and that it is acceptable to choose this thickness based on other criteria.

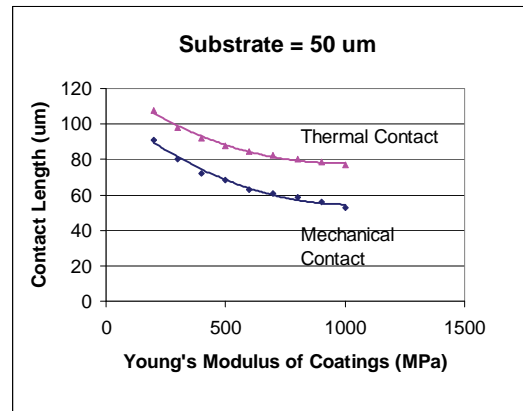


**Figure 8.** Dependence of contact-length on the Young's modulus Y\_coatings of the thermally active coatings.

The same claim can be made regarding the thickness of the adhesive. It is preferable that this thickness is small, and Figure 9 illustrates the dependence of heater contact-length on this parameter for several values of Y\_coatings

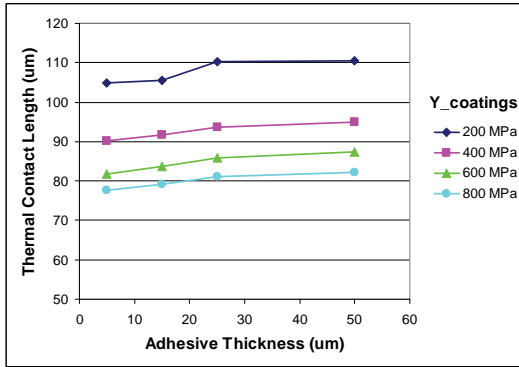


**Figure 9.** Thermal contact length as a function of adhesive thickness. In this analysis,  $Y_{\text{adhesive}} = 100 \text{ MPa}$  and  $Y_{\text{substrate}} = 2.3 \text{ GPa}$ .

From this figure, it can be seen that the dependence of thermal contact-length on adhesive thickness is quite mild, and the principal determining factors for contact-length are actually the Young's moduli of the coatings and the substrate.

Despite the fact that most non-voided plastic substrates available for coating have a Young's modulus in the range of 2-3 GPa, we carried out a study of the effect of substrate stiffness on contact-length. The coatings and adhesive in this study were given Young's moduli of 800 MPa and 300 MPa respectively, and the results are shown in Figure 10.

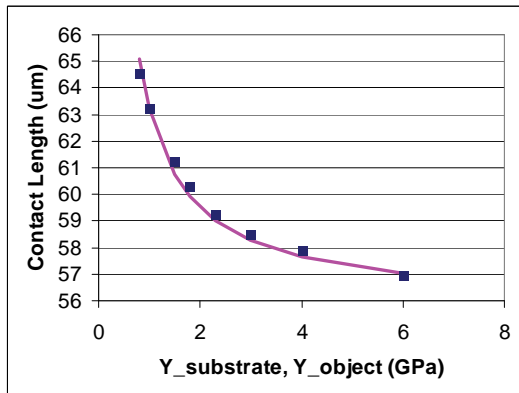


**Figure 10.** Variation of contact-length with  $Y_{\text{substrate}}$ , with fixed values of  $Y_{\text{adhesive}}=300 \text{ MPa}$  and  $Y_{\text{coatings}}=800 \text{ MPa}$ .

The results of study were well-described by a function of the form:

$$f(Y_{\text{substrate}}) = A + B/Y_{\text{substrate}},$$

where  $A=55.8 \text{ um}$ . This means that in the limit of a very stiff substrate, there is still a non-zero contact-length. This results from the compliance of the coatings and argues for keeping the coating materials, themselves, as compliant as possible. Any additional contacts that may be gained by variations in the substrate or adhesive are supplemental to this base level of contact.

Finally, studied the dependence of contact-length on position along the print head. This was done by making a 2D graph of the contact parameter vs. position on the glass bump, and finding the boundary between contact and non-contact. The boundary is noisy, due to the rather coarse mesh, but fit well to a function of the form  $f(x)=A-B*\exp(x/C)$  as shown in Figure 11, where  $x$  is the distance from the edge of the print head. In this example, the fitted parameters are  $A=29.6 \text{ um}$ ,  $B=3.7 \text{ um}$  and  $C=19.3 \text{ um}$ . These results indicate that at the edge of the print head, the contact length is  $2*(A-B)=52 \text{ um}$ , and it increases to a contact length of  $2*A=59 \text{ um}$  over a characteristic distance of about 19 um. Thus the "end-effect" for contact-length is somewhat more confined than that for compressibility.

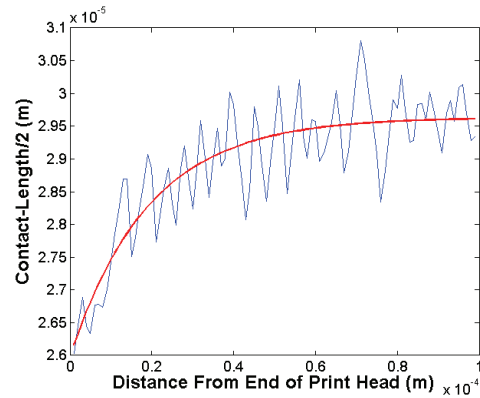


**Figure 11.** Contact length as a function of distance from the end of the print head. In this example,  $Y_{\text{coatings}}=800 \text{ MPa}$ ,  $Y_{\text{adhesive}}=300 \text{ MPa}$ , and  $Y_{\text{substrate}}=2.3 \text{ GPa}$ .



### 3.2 Patterned Adhesive

In order to build additional compressibility into the structure, we also investigated the possibility of using a “distributed adhesive”. In this model, the adhesive was represented as pillars surrounded by air, as shown in Figure 12.

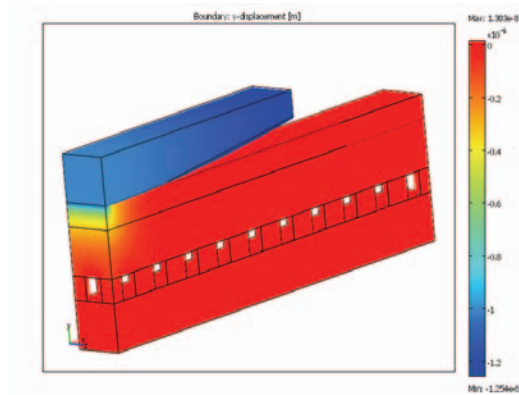


**Figure 12.** Schematic representation of the model with a distributed adhesive layer. The adhesive forms of an array of cylinders separated by air gaps.

Figure 13 shows the results from a typical study in which the adhesive cylinders had a radius of 20 microns and a pitch of 50 microns. As in earlier studies the substrate and adhesive had Young’s moduli of 2.3 GPa and 100 MPa respectively. The Young’s modulus of the coatings was varied from 0.1-1.0 GPa.

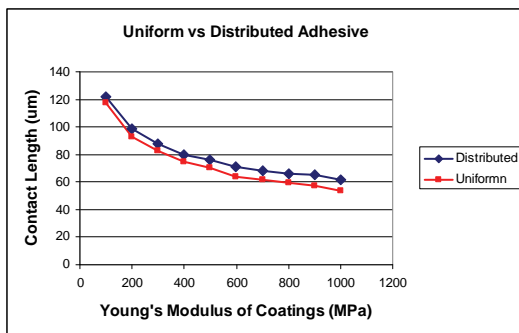


**Figure 13.** Comparison of contact-length for a reference structure with uniform adhesive, and a modified structure having distributed dots of adhesive. The dots were cylinders of radius 20 microns, and a pitch of 50 microns.

Over this range of parameters, we found that the additional contact achieved by distributing the adhesive was only a small increment to that already available from the native compliance of the coatings themselves.

### 4. Conclusions

We have produced a model of multilayer thermal printing materials for the purpose of evaluating the use compressible adhesives to obtain improved wrapping of the print media around the heating elements. Results were obtained for a range of Young’s moduli for the thermally active coatings, the adhesive and the substrate.

It was found that fast computations for the performance over most of the print head can be achieved by using a simpler 2D plane-strain model, though that model becomes inaccurate within 100-200 um of the end of the print head.

The results for heater contact-length were found to be relatively insensitive to the thickness of the adhesive and the substrate, but to depend more strongly on the Young’s modulus of the substrate and active coatings. The picture that emerges is that a soft adhesive functions as a cushion for the label, affecting the overall compressibility but not contributing significantly to the wrap of the media around the glass bump. The thermally active coatings were found to provide a certain base level of contact-length, based on their native compliance, even when applied to a very stiff substrate. This level of contact can be improved moderately by reducing the stiffness of the substrate, though the values of Young’s modulus required are not characteristic of usual substrate materials.

### 5. References

1. S. Telfer and W. T. Vetterling, *A New, Full-Color Direct Thermal Imaging System*, Proc. of the NIP21 Non-Impact Printing Conf., Baltimore (2005).
2. W. T. Vetterling, B. Busch and C. Liu, *A Model of Direct Thermal Printing*, Proc. of the 2007 COMSOL Conference, Newton, MA.
3. S. Timoshenko, *Theory of Elasticity*, Chap. 2, McGraw-Hill, New York (1970).